Variable turbulent Prandtl number model applied to hypersonic shock/boundary-layer interactions

Subhajit Roy* and Krishnendu Sinha†
Indian Institute of Technology Bombay, Mumbai 400076

Interaction of shock waves with turbulent boundary-layers can enhance the surface heat flux dramatically. Reynolds-averaged Navier-Stokes simulations based on constant turbulent Prandtl number often give grossly erroneous heat transfer predictions in SBLI flows. This is due to the fact that the underlying Morkovin's hypothesis breaks down in the presence of shock waves; thus, the turbulent Prandtl number can not be assumed to be a constant. In our recent work (Roy, Pathak and Sinha,AIAA 2017), we developed a new variable turbulent Prandtl number model based on linearized Rankine-Hugoniot conditions applied to shock-turbulence interaction. The turbulent Prandtl number is a function of the shock strength and we proposed a shock function to identify the location and strength of shock waves. The shock function also simulates the post-shock ralaxation of the turbulent heat flux, akin to that observed in canonical shock-turbulence interaction. In this work, we extend the variable turbulent Prandtl number model for hypersonic flows by considering the influence of upstream total temperature fluctuation on turbulent heat flux. The model is combined with the well-validated shock-unsteadiness k-ω model and is used to study eight test cases involving shock/boundary-layer interactions at Mach numbers ranging from 5 to 11. Comparison with experimental data shows significant improvement in the surface heat transfer rate in the interaction region. The shock function is also used to propose a robust form of the existing shock-unsteadiness k-ω model that simplifies the numerical implementation enormously.

Nomenclature

Pr_T	Turbulent Prandtl number
P_k	Production term of turbulent kinetic energy
S_{ij}	Symmetric part of mean strain rate tensor
S_{ii}	Mean dilatation
b_1'	Shock-unsteadiness damping parameter
A_{uT}	Correlation between temperature and velocity fluctuations
r	Density ratio
c_f	Skin friction co-efficient
q_w	Wall heat flux, W/cm^2
δ_0	Boundary-layer thickness upstream of interaction, m
k	Turbulent kinetic energy, m^2/s^2
ω	Specific dissipation rate of turbulent kinetic energy, s^{-1}
ξ_t	Instantaneous shock speed, m/s
ψ	Shock function

Subscript

∞	Free-stream condition
w	Wall condition

*Doctoral student, Department of Aerospace Engineering.
†Professor, Department of Aerospace Engineering, Senior AIAA Member.

I. Introduction

Shock/boundary-layer interactions (SBLIs) are commonly observed in high-speed flows and they are characterized by a rise in surface pressure and high localized heat transfer. Accurate prediction of surface properties becomes important for high-value aerospace applications. A considerable number of studies have investigated SBLIs occurring in varying conditions and configurations.[1] CFD simulations through Reynolds-averaged Navier-Stokes (RANS) based turbulence models are popular in the aerospace industry. Current turbulence models, however, over-predict the peak heat flux values by considerable margins,[2,3] and in this work we systematically study and tackle this problem for hypersonic flows.

Transport of heat in standard turbulence models is modeled through temperature gradient approximation, with thermal conductivity having molecular and turbulent components. The turbulent part of thermal conductivity is usually written in terms of the turbulent Prandtl number (Pr_T), which is calculated based on Morkovin's hypothesis.[4] A direct mathematical implication of Morkovin's hypothesis is the Strong Reynolds Analogy. It states that the value of velocity-temperature correlation coefficient is -1, which leads to a theoretical value of $Pr_T = 1$. A value of 0.89 produces results that are in good agreement with the experimental data for turbulent boundary layers. This is not the case for SBLI flows, where the ability of the constant Pr_T approach has been called into question by several authors in the past.[5]

A natural progression in the modeling of turbulent heat flux is therefore to vary the Pr_T. Variable Pr_T models have shown improvement in the heat flux predictions in SBLI flows.[6,7] Most of the variable Pr_T models solve two additional transport equations for temperature variance and its dissipation rate. The turbulent Prandtl number is then calculated using the time scale of the temperature variance. The additional partial differential equations have a form similar to the k-ϵ or k-ω equations, and have a large number of source terms. The solution of extra equations thus requires more computational power and invariably increases the cost of computation. Algebraic Pr_T models have been devised to account the Pr_T variation in boundary layers, but they do not consider the effect of shocks.[8] In fact, recent studies of shock-turbulence interaction[9,10] have revealed interesting and non-intuitive variation of the turbulent heat flux across shock waves. The underlying physical mechanisms should, therefore, be considered for computing the turbulent Prandtl number in SBLI flows.

In a recent work Roy, Pathak and Sinha[11] proposed a new method to vary Pr_T based on the physics of shock-turbulence interaction and subsequently extended the model to SBLI flows. They derived a relationship between the fluctuating velocity and temperature behind a shock, which is used to develop an expression for Pr_T as a function of shock strength. A novel approach is presented to identify the location and strength of shock waves at every grid point in term of a shock function. The shock function is computed by solving a differential equation. The transport equation of shock function also incorporates an exponential relaxation of the turbulent Prandtl number from its shock value to the conventional value of 0.89 away from the shock wave. The variable turbulent Prandtl number model of Roy, Pathak and Sinha[11] is built upon the previously developed shock-unsteadiness (SU) turbulence model.[12] Compared to conventional models, the shock-unsteadiness correction eliminates the over-amplification of turbulent kinetic energy (TKE) at shock waves. It gives significant improvement in predicting the separation bubble size and the surface pressure distribution in SBLI flows.[13] The computed shock/expansion wave patterns and shock-shock interaction match experimental data closely.[14,15] Due to its potential, the shock-unsteadiness model has been used widely[16,17] and is being developed further in recent works.[11,18,19] The variable Pr_T model, in conjunction with the shock-unsteadiness k-ω model, is found to reproduce the experimental data of Schulein[20] well for Mach 5 oblique shock impinging cases.

The variable turbulent Prandtl number model of Roy, Pathak and Sinha[11] is build upon the assumption that Morkovin's[4] hypothesis is valid upstream of the shock wave and they have neglected the upstream fluctuations of total temperature. This is a fair assumption upto a moderate Mach number of 5, i.e. for a supersonic turbulent boundary layer, but beyond this Mach number the assumption is not fully valid. There has been a lot of experimental and numerical data available in the literature[21,22] to support the breakdown of this assumption. In this work, we extend the variable Pr_T model of Roy, Pathak and Sinha[11] for hypersonic flows and considered the effect of upstream total temperature fluctuations also. We followed the same procedure and study the fundamental interaction of homogeneous isotropic turbulence with a shock wave first, commonly known as shock-turbulence interaction (STI). The theoretical tool called linear interaction analysis (LIA) is used to investigate the STI problem. We develop a more general formulation of Pr_T based on this theoretical analysis which is applicable for any Mach number. Similar to our previous work,[11] the local SU k-ω model has been used as a baseline model for this work.

This article is organised as follows. The next section describes the experimental SBLI configurations and test conditions of Holden et al.,[23,24] which are used to validate the proposed model. A brief review of the governing equations are presented in following section along with the numerical method and boundary conditions used in the simulations. Next, we extend the variable turbulent Prandtl number model (Roy, Pathak and Sinha, AIAA 2017) for hypersonic flows based on the shock turbulence interaction physics. We also present the shock -unsteadiness modified k-ω model in this section. The local form of the shock-unsteadiness modification (Roy, Pathak and Sinha, AIAA 2017) is used for all the simulations. This local form reduces the total computation time and susceptibility to human error significantly. The last section presents computed results and these are compared with the experimental data to bring out the differences between the predictions of standard k-ω, shock-unsteadiness k-ω and variable turbulent Prandtl number models.

II. Test Cases

The test cases presented here are all two-dimensional or axisymmetric. Three different geometric configurations, compression ramp, Oblique shock impinging on a flat plate and axisymmetric cone-flare, are considered to evaluate the variable Pr_T model at hypersonic Mach numbers. All the experiments were performed by Holden et al.[23–25] in the CUBRC. For all the experiments the surface temperature is maintained under isothermal condition. The schematic of the experimental configurations for different geometries can be seen in Fig 1.

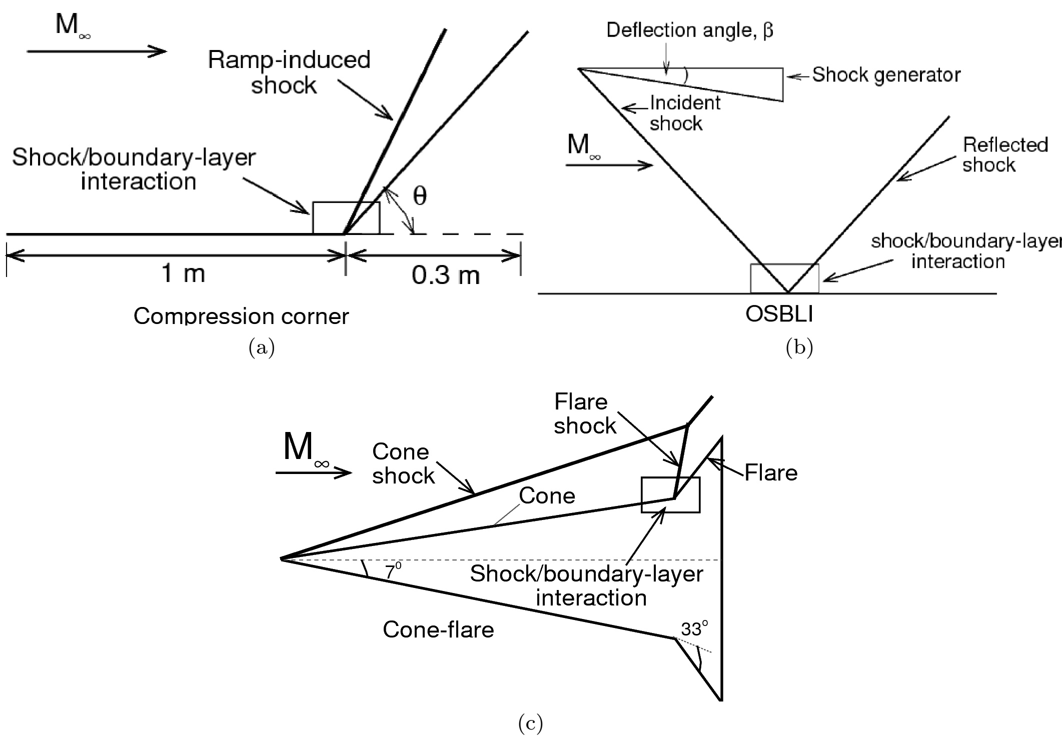

Figure 1. Experimental configuration for (a) compression corner, (b) oblique shock impinging on a flat plate and (c) cone-flare geometries.[23,24]

The test conditions for different configurations are tabulated in table 1. For the compression corner test cases, the length of flat plate is almost 1m before the corner, followed by a 0.3m wedge. The length of the flat plate is long enough to get a fully developed turbulent boundary-layer ahead of the interaction region. The experimental configuration of oblique shock impingement consists of a flate (1.27m long) and a shock generator with a deflection angle β=20 degree. The flat plate was kept in the center of test section, whereas the shock generator was placed axially above the plate such that the inviscid shock impinged at a location of 0.98m from the plate leading edge. The length of cone and flare along center line axis from the cone tip are measured as 2.35 m and 0.15 m respectively. Surface properties like pressure and heat flux were measured in the interaction region. For all the experiments dry air is taken as the working fluid with perfect gas assumption.

Table 1. Test conditions

Hypersonic Experiments	M_∞	ρ_∞ (kg/m^3)	T_∞ (K)	Deflection Angles	T_w (K)	$H_{0,\infty}$ (MJ/kg)	ReU_∞/m
Compression Corner	11.3	0.08246	61	36^o	300	1.63	36×10^6
	8.2	0.4990	70	36^o	298	1.02	145×10^6
	8.1	0.4910	71.7	33^o	297	1.02	139×10^6
Oblique shock impinging	11.4	0.08910	63	20^o	300	1.71	38×10^6
Cone-flare	8.21	0.0437	60.4				
	8.21	0.0437	60.4	7^o & 40^o	306.5	0.88	33.5×10^6
	7.18	0.0572	66.6	7^o & 40^o	302.5	0.76	36.6×10^6
	6.17	0.0737	56.7	7^o & 40^o	297.4	0.49	44.3×10^6
	5.1	0.284	75.8 K	7^o & 40^o	294.6	0.47	118×10^6

III. Simulation methodology

We solve the two-dimensional or axisymmetric Reynolds-averaged Navier-Stokes equations presented by Wilcox[5] for the mean flow. The two-equation k-ω model of Wilcox[5] and the recent shock-unsteadiness corrected k-ω model of Sinha et al.[13] are used in the simulations. Both the standard and shock-unsteadiness corrected k-ω models do not include any compressibility corrections,, as they are found to deteriorate model predictions in the undisturbed boundary layer upstream of the interaction.[26,27] Compressibility corrections of the form of dilatational dissipation reduce the turbulent kinetic energy in the boundary layer, and thus decrease the skin friction coefficient compared to well-established correlations for zero pressure-gradient turbulent boundary layers.

The governing equations are discretised in a finite volume formulation where the inviscid fluxes are computed using a modified, low-dissipation form of the Steger-Warming flux splitting approach.[28] This method reduces the numerical dissipation, and is found to be useful for high-speed flows with strong shock waves and viscous-inviscid interactions with boundary layers. As a result, very thin and well-defined shock waves are captured over a few grid cells. The turbulence model equations are fully coupled to the mean flow equations. The details of the formulation are given by Sinha and Candler.[29] The method is second-order accurate in space. The viscous fluxes and the turbulent source terms are evaluated using second-order accurate central difference method. The implicit Data Parallel Line Relaxation method of Wright et al.[30] is used to integrate in time and reach steady-state solution.

At the wall, isothermal temperature and no-slip boundary conditions are applied, and extrapolation condition is used at the exit boundary of the domain for all the simulations. A supersonic boundary condition is imposed at the top boundary of the domain. For the turbulence quantities, the boundary conditions at the wall (Menter 1994)[31] are taken as $k = 0$ and $\omega = 60\nu_w/\beta_1\Delta y_1^2$, where ν_w is kinematic viscosity at the wall, $\beta_1 = 3/40$ and Δy_1 is the normal distance to the grid point nearest to the wall. Following Menter,[31] the freestream conditions used for all the simulations are $\omega_\infty = 10U_\infty/L$ and $k_\infty = 0.01\nu_\infty\omega_\infty$ where L = 1 m is a characteristic length of the geometry.

IV. Variable Turbulent Prandtl Number Model

Generally, the turbulent heat flux vector $q_{T,j}$ is modeled using the gradient diffusion hypothesis

$$q_{T,j} = -\kappa_T \frac{\partial \overline{T}}{\partial x_j}, \tag{1}$$

where κ_T is the turbulent conductivity of heat. It is related to eddy viscosity via the turbulent Prandtl number Pr_T and the specific heat of the gas at constant pressure c_p.

$$\kappa_T = \frac{\mu_T c_p}{Pr_T} \tag{2}$$

Morkovin hypothesis[4] relates the turbulent heat flux to the Reynolds stress in a compressible turbulent boundary layer and thus prescribes a constant value of the turbulent Prandtl number. However, the assumption of zero total temperature fluctuation in Morkovin hypothesis[4] is not valid across a shock wave where a constant value of turbulent Prandtl number is not desirable.

Variation of turbulent Prandtl number improves the heat flux prediction capabilities of standard turbulence models significantly. In a recent work, Roy, Pathak and Sinha[11] developed an algebraic variable Pr_T model based on the shock-turbulence interaction physics. The shock-normal Reynolds stress is modeled in terms of the Boussinesq approximation whereas the conservation of total enthalpy is used to model the shock-normal turbulent heat flux behind the shock wave. The shock wave undergoes unsteady motion in response to the fluctuations in a turbulent flow. The deviation of the shock from its mean position is taken as $\xi(y, z, t)$, such that the temporal derivative ξ_t represents the instantaneous shock speed in the streamwise direction.[32] The total temperature in the shock reference frame is written as

$$T_0 = \overline{T} + T' + \frac{(\overline{u} + u' - \xi_t)^2 + v'^2 + w'^2}{2c_p} \tag{3}$$

Here, u,v,w are the velocity components, overbar represents mean flow quantity and primes denote turbulent fluctuations. Assuming the shock speed and fluctuations to be small as compared to the jumps in the mean flow quantities across the shock, the linearized total temperature consevation across the shock is given as:

$$T_1' + \frac{\overline{u_1} u_1'}{c_p} = T_2' + \frac{\overline{u_2} u_2'}{c_p} + \frac{\xi_t}{c_p}(\overline{u_1} - \overline{u_2}), \tag{4}$$

where 1 and 2 denote the shock upstream and downstream location respectively. The left-hand side of the above equation represents the linearized form of the total temperature fluctuations upstream of the shock wave. Roy, Pathak and Sinha[11] assumed the total temperature fluctions to be negilible in the upstream flow. This is a fair assumption for a supersonic undisturbed turbulent boundary-layer. Hence the turbulent heat flux behind the shock wave is given as

$$\overline{u'T'} = -\frac{\overline{u}}{c_p}\left(\overline{u'^2} + \overline{u'\xi_t}(r-1)\right), \tag{5}$$

where r is the mean density ratio across the shock wave. The unclosed correlation $\overline{u'\xi_t}$ is modeled as per the shock-unsteadiness model of Sinha et al.[12]

$$\overline{u'\xi_t} = b_1 \overline{u'^2} \quad \text{with} \quad b_1 = 0.4 + 0.6e^{2(1-M_1)} \tag{6}$$

The above equation is based on the assumption that the unsteady shock motion is caused by the incoming turbulent velocity fluctuations, and the closure coefficient b_1 is obtained from linear interaction analysis. The aforementioned model accounts only the shock motion at frequencies comparable to that of the incoming turbulence. Additional low-frequency shock oscillations, observed in the SBLI, have a negligible correlation with the turbulent velocity fluctuations in the boundary layer. Such low frequency shock motion do not contribute to the $\overline{u'\xi_t}$ correlation. We thus get

$$\overline{u'T'} = -\frac{\overline{u}}{c_p}\overline{u'^2}\left(1 + b_1(r-1)\right), \tag{7}$$

and the turbulent Prandtl number is given as

$$Pr_T = \frac{\mu_T c_p}{\kappa_T} = \frac{3}{4}\frac{\overline{u'^2}}{\overline{u'T'}}\frac{\partial \overline{T}}{\partial x}\left(\frac{\partial \overline{u}}{\partial x}\right)^{-1} = \frac{3}{4}\left(\frac{1}{1 + b_1(r-1)}\right) \tag{8}$$

The above formulation of turbulent Prandtl number is applicable for supersonic flows where the total temperature fluctuation is negligible in the undisturbed turbulent boundary layers, as per Morkovin hypothesis.[4]

A. Extension to hypersonic flows

The applicability of Morkovin's hypothesis[4] has been called into question by several researcher in last decade. Leschziner[21] and Duan[22] suggest that the amount of total temperature fluctuations T_t' can be neglected up to a moderate Mach number 5, but T_t' is comparable to static temperature fluctuations T' and it can not be neglected in hypersonic flows. In the current work, we consider the effect of upstream total temperature fluctuations, given by

$$T_t' = T_1' + \frac{\overline{u_1} u_1'}{c_p} \neq 0, \tag{9}$$

and exend the variable Pr_T model for hypersonic flows. The modification is done in two steps. First we consider the effect of upstream velocity fluctuations and model the effect in the vicinity of shock wave. Next we consider the effect of both velocity and temperature fluctuations upstream of the shock wave to model the turbulent Prandtl number across shock waves.

1. *Effect of upstream velocity fluctuation:*

For purely vortical turbulence upstream of the shock wave, we have all the thermodynamic fluctuations are negligible before the shock, i.e. $T_1' \to 0$, which leads to (see Eq. 4)

$$T_2' + \frac{\overline{u_2} u_2'}{c_p} = \frac{\overline{u_1} u_1'}{c_p} - \frac{\xi_t}{c_p}(\overline{u_1} - \overline{u_2}) \tag{10}$$

On taking a moment with u_2', we get

$$\overline{u_2' T_2'} = -\frac{\overline{u_2}}{c_p}\left(\overline{u_2'^2} + \overline{u_2' \xi_t}(r-1) - r\overline{u_1' u_2'}\right) \tag{11}$$

Compared to earlier model, the right-hand side has the additional contribution from the upstream velocity fluctuation u_1'. The unclosed correlation between the upstream and downstream velocity fluctuations is modeled in terms of the parameter α; see Ref.[11]

$$\overline{u_1' u_2'} \sim \alpha \overline{u_2'^2} \tag{12}$$

and unsteady shock speed is modeled as per Eq. (6) to get

$$\overline{u'T'} = \frac{\overline{u}}{c_p}\overline{u'^2}\left[(r\alpha - 1) - (r-1)b_1\right], \tag{13}$$

where the subscript 2 is dropped for convenience. The above form is identical to Eq. (7) except for the α-term. Hence the turbulent Prandtl number is given as

$$Pr_T = \frac{3}{4}\left(\frac{1}{b_1(r-1) - (r\alpha - 1)}\right). \tag{14}$$

A value of $\alpha = 0.6$ matches the DNS data of Larson et al.[33] fairly well over the entire range of Mach numbers.[11]

2. *Effect of upstream total temperature fluctuation:*

We next include the effect of both temperature and velocity fluctuations that contribute to the total temperature fluctuations in the upstream boundary layer. We follow the work of Sinha[32] where a correlation function A_{uT} is defined to relate the velocity and temperature fluctuations in the flow.

$$-\frac{T'}{\overline{T}} = A_{uT}\frac{u'}{\overline{u}} \tag{15}$$

A_{uT} can be interpreted as the ratio of normalized temperature and velocity fluctuations. A general expression for A_{uT} in a turbulent boundary layer is given as; see Appendix A for details:

$$A_{uT} = -(\gamma - 1)M^2 \frac{R_{uT}}{Pr_T}\left(\frac{\partial \overline{T_t}}{\partial \overline{T}} - 1\right)^{-1} \tag{16}$$

where M is the local Mach number, $\overline{T_t}$ and $\overline{T}$ are mean total and static temperature respectively. $R_{uT} = \overline{u'T'}/(\sqrt{\overline{u'^2}}\sqrt{\overline{T'^2}})$ is the correlation coefficient between streamwise velocity and temperature fluctuations. The boundary layer data presented by Guarini[34] show that the value of $R_{uT} \simeq -0.6$ for $0.2< y/\delta <0.8$ and it attains higher magnitude of -0.8 in the near wall region. The value of R_{uT} falls off to negligible values at the boundary-layer edge. A similar trend is reported by Pirozzoli et al.[35] for a turbulent boundary-layer at Mach 2.25 and Gaviglio[36] for a turbulent boundary-layer at Mach 9.4. Based on our previous work[37] we highlighted that the log-region ($0.05< y/\delta <0.25$) of boundary-layer is most important to model wall heat flux and we take an average value of $R_{uT} = -0.7$ in our current simulations.

We follow the procedure laid out earlier and start with Eq. (4). We substitute Eq. (15) to get

$$-A_{uT}u_1'\frac{\overline{T_1}}{\overline{u_1}} + \frac{\overline{u_1}u_1'}{c_p} = T_2' + \frac{\overline{u_2}u_2'}{c_p} + \frac{\xi_t}{c_p}(\overline{u_1} - \overline{u_2}) \tag{17}$$

On taking a moment with u_2', we get

$$\overline{u_2'T_2'} = -\frac{\overline{u_2}}{c_p}\left(\overline{u_2'^2} + \overline{u_2'\xi_t}(r-1) - r\overline{u_1'u_2'} + A_{uT}c_p\frac{1}{rT_r}\frac{\overline{T_2}}{\overline{u_2}^2}\overline{u_1'u_2'}\right) \tag{18}$$

Compared to earlier model formulation, the right-hand side has the additional contribution from the upstream the upstream velocity fluctuation u_1' and upstream temperature fluctuations (the A_{uT} term). Here $T_r = \overline{T_2}/\overline{T_1}$ is the mean temperature ratio across shock wave. Using Eqs. (6) and (12) we get

$$\overline{u'T'} = -\frac{\overline{u}}{c_p}\overline{u'^2}\left[(1+(r-1)b_1 - \alpha r + \frac{\alpha A_{uT}}{(\gamma-1)M^2}\frac{1}{rT_r}\right], \tag{19}$$

where the subscript 2 is dropped once again for convenience. The above form is identical to Eq. (7) except two additional terms in the right hand side which bring the effect of upstream total temperature fluctuations in the model. Substitution into Eq. (8) leads to,

$$Pr_T = \frac{3}{4}\frac{1}{1 + b_1(r-1) + \dfrac{\alpha A_{uT}}{(\gamma-1)M^2}\dfrac{1}{rT_r} - \alpha r} \tag{20}$$

The additional two terms in the above equation almost cancel each other in supersonic flow, which is consistent with negligible total temperature fluctuations in such flows.

B. Shock function formulation

Roy, Pathak and Sinha[11] composed a transport equation for a scalar shock function ψ to evaluate the mean density ratio at the shock region. The turbulent Prandtl number is then modeled in terms of ψ. The transport equation for ψ is such that ψ deviates from its undisturbed value ψ_0 only in the regions of strong compression and gradually relaxes back from the shock value to the reference value.

$$\frac{\partial(\overline{\rho}\psi)}{\partial t} + \frac{\partial(\overline{\rho}\widetilde{u_i}\psi)}{\partial x_i} = \overline{\rho}\psi S_{ii} - \overline{\rho}(\psi - \psi_0)\frac{\sqrt{\widetilde{u_i}\widetilde{u_i}}}{L_\epsilon}, \tag{21}$$

where $S_{ii} = \frac{\partial \widetilde{u_i}}{\partial x_i}$ is the mean dilatation, $\sqrt{\widetilde{u_i}\widetilde{u_i}}$ is the velocity magnitude and $L_\epsilon = \sqrt{k}/\omega$ is the dissipation length scale in the k-ω framework. Integrating the differential equation across a shock gives the shock value ψ_s as

$$\frac{\psi_s}{\psi_0} = \frac{\overline{u_2}}{\overline{u_1}} = \frac{1}{r} \tag{22}$$

Thus, ψ_s is an indicator of the shock strength and an upstream undisturbed value of $\psi_0 = 1$ ensures that we get $\psi_s = 1/r$ at the shock location.

Substitution of $r = 1/\psi$ in Eq. (8) gives an expression for turbulent Prandtl number as

$$Pr_T = \frac{3}{4}\frac{\zeta}{1 + b_1(r-1) + \dfrac{\alpha A_{uT}}{(\gamma-1)M^2}\dfrac{1}{rT_r} - \alpha r} \tag{23}$$

where an additional factor ζ is introduced to make the formulation consistent with the conventionally accepted Pr_T value of 0.89 in boundary layers without shock waves. For vanishing shock strength in the limit $M_1 \to 1$, r $\to 1$ and $\psi \to 1$, Pr_T should take a value of 0.89. Thus, ζ is defined as

$$\zeta = 1 + \left(\frac{0.89}{0.75} \left(1 + \frac{\alpha A_{uT}}{(\gamma - 1)M^2} - \alpha \right) - 1 \right) exp \left(\chi (1 - \frac{1}{\psi}) \right). \tag{24}$$

such that it approaches 1 in the presence of shock waves. Here χ is model parameter and its value is equal to 1000; see Roy, Pathak and Sinha[11] for more details.

C. Shock-unsteadiness modified k-ω model

The variable Pr_T model presented above is implemented in the shock-unsteadiness (SU) modified k-ω model. The shock unsteadiness model was first proposed by Sinha et al.[12] and was subsequently incorporated in one- and two-equation turbulence models.[13] The original shock-unsteadiness model[12] considered only the influence of upstream velocity fluctuation on shock wave. Later, Veera and Sinha[38] incorporated the effect of upstream temperature fluctuation on shock-unsteadiness model. For easy reference, the highlights of the model and its implementation in the k-ω framework are presented here.

In the k-ω model, the production of turbulent kinetic energy is given by:

$$P_k = \mu_T \left(2S_{ij}S_{ji} - \frac{2}{3}S_{ii}^2 \right) - \frac{2}{3}\bar{\rho}kS_{ii} \tag{25}$$

where $S_{ij} = \frac{1}{2}\left(\partial\widetilde{u_i}/\partial x_j + \partial\widetilde{u_j}/\partial x_i\right)$ is the mean strain rate tensor and $\widetilde{u_i}$ is the component of the Favre-averaged velocity in the x_i direction. The eddy viscosity is given by $\mu_T = \rho k/\omega$. Sinha et al.[12] argue that the eddy viscosity assumption breaks down in the highly non-equilibrium flow through a shock and a more accurate amplification of k is obtained by setting $\mu_T = 0$ in the production of turbulent kinetic energy. Based on linear analysis results, they propose the following modification to the production term in a shock wave,

$$P_k^{'} = -\frac{2}{3}\bar{\rho}kS_{ii} \left(1 - b_1^{'} + \frac{A_{uT}}{2}(1 + \frac{1}{T_r}) \right). \tag{26}$$

The shock-unsteadiness correction is applied in the k-ω framework by multiplying the eddy viscosity of the standard model by the factor,

$$c_\mu^{'} = 1 - f_s \left[1 + \frac{\left(b_1^{'} - \frac{A_{uT}}{2}(1 + \frac{1}{T_r}) \right)}{\sqrt{3}S/\omega} \right]$$

where $S = \left[2S_{ij}S_{ji} - \frac{2}{3}S_{ii}^2\right]^{1/2}$ and f_s is an empirical function of the non-dimensional mean dilatation $S_{ii}\delta_0/U_\infty$,[14]

$$f_s = \frac{1}{2} - \frac{1}{2}\tanh\left[12\left(S_{ii}\delta_0/U_\infty\right) + 4\right] \tag{27}$$

It takes a value of one in shock and high compression regions, such that $c_\mu^{'} = -\left(b_1^{'} - \frac{A_{uT}}{2}(1 + \frac{1}{T_r}) \right) / \sqrt{3}(S/\omega)$, otherwise it is zero and the standard form of k-ω model is recovered.

The shock function is used to implement the shock-unsteadiness model locally in a numerical code. The upstream shock-normal Mach number dependence of the model parameters (see Sinha et al.[12] for more details) b_1 and b_1' are replaced by the local density ratio. The local density ratio r represents the shock strength and thus the flow-physics captured by the original shock-unsteadiness model remain unchanged. the shock-unsteadiness parameters are recast as

$$b_1' = (0.4 + 0.2A_{uT}) \left(\frac{r - 1}{5} \right)^{0.3} = (0.4 + 0.2A_{uT}) \left(\frac{1 - \psi}{5\psi} \right)^{0.3} \tag{28}$$

$$b_1 = (0.4 + 0.2A_{uT}) + 0.6 \left(\frac{6 - r}{5} \right)^{5.2} = (0.4 + 0.2A_{uT}) + 0.6 \left(\frac{6\psi - 1}{5\psi} \right)^{5.2}. \tag{29}$$

The exponents in Eqs. (28) and)(29) are obtained by curve fitting to the original model coefficients b_1 and b_1' from.[12,38] The shock function is also used to compute the mean temperature ratio T_r across shock waves.

V. Results

The new variable Pr_T model is applied to three different geometries with SBLI. Eight test cases with Mach number ranging from 5 to 11 are presented in this section. The effect of the variable Pr_T model on the surface properties are compared with existing turbulence models. The detail of the grid refinement is not presented here as the procedure is similar to those presented in Roy, Pathak and Sinha. The new variable Pr_T model is used to study the grid convergence for the current test cases and based on that 340×250, 500×350 and 700×350 grid points are used for compression corner, oblique shock impinging on a flat plate and cone-flare geometries respectively. For all the simulations a wall-normal spacing of 1×10^{-6}m are used for the first cell center in the interaction region. This corresponds to a y_2^+ value of 0.4 or lower in the interaction region.

A. Compression corner

To save the computation time the flat plate length before the corner is reduced to 0.2m compared to 1m length in the experiment (see Fig. 1). The domain consists of a 0.2m long flat plate followed by a 0.3m ramp and it extends to 0.06m above the plate where an inlet profile is specified at the starting of the domain. Inlet profiles for the compression ramp computations are obtained from separate flat plate simulation with same free stream and wall boundary conditions as mentioned in table 1.

Figure 2 shows the flow field solution computed for an SBLI generated by the 33 degree compression corner at Mach 8.1. The shock topology is presented in terms of the mean density contours. The solution corresponds to the SU k-ω turbulence model with the variable Pr_T formulation. The key features of the interaction region are identified in terms of the separation shock, reattachment shock and the ramp-induced shock. The SU k-ω model also captured the free shear-layer at the shock-shock interaction point around $x = 0.03m$. The computed shock structure is compared with the experimental schlieren image;[23] see Fig. 2(b). The computed shock structure is found to match the experimental image qualitatively.

Figure 3 compares the computed surface properties with the experimental data reported by Holden.[23] Three turbulence models are used in the simulations, namely, the standard k-ω model, the shock-unsteadiness k-ω and the variable Pr_T formulation added to the shock-unsteadiness k-ω model. Surface pressure shows a jump at the separation point (at $x = -0.019$m), followed by a small pressure plateau and a subsequent increase at the reattachment point. The computed results match the experimental measurements, except for the pressure far away from the compression corner. All the three turbulence models have almost identical results, with a small deviation in the vicinity of the separation point. The variable Pr_T form of the SU k-ω model predicts identical surface pressure as that of the constant Pr_T version.

The heat flux data shows a trend similar to the surface pressure, with a constant value in the undisturbed boundary-layer and a rise in the heat transfer rate at the separation point which mimic the experimental trend closely. The standard k-ω model, however, overpredicts the heat flux by about 50%. The shock-unsteadiness correction is found to reduce the surface heat transfer rate, but the results are still substantially higher

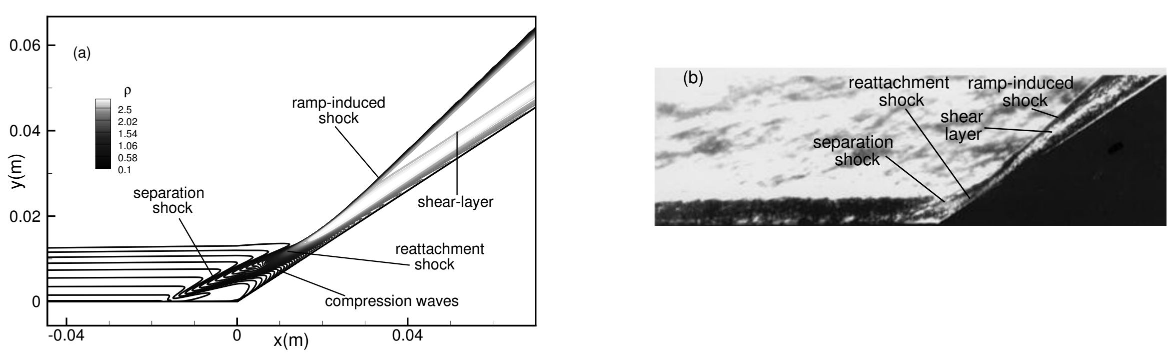

Figure 2. Comparison of (a) computed density contours using SU k-ω model and (b) experimental schlieren image[23] for $\theta = 33^o$ and $M_\infty = 8.1$.

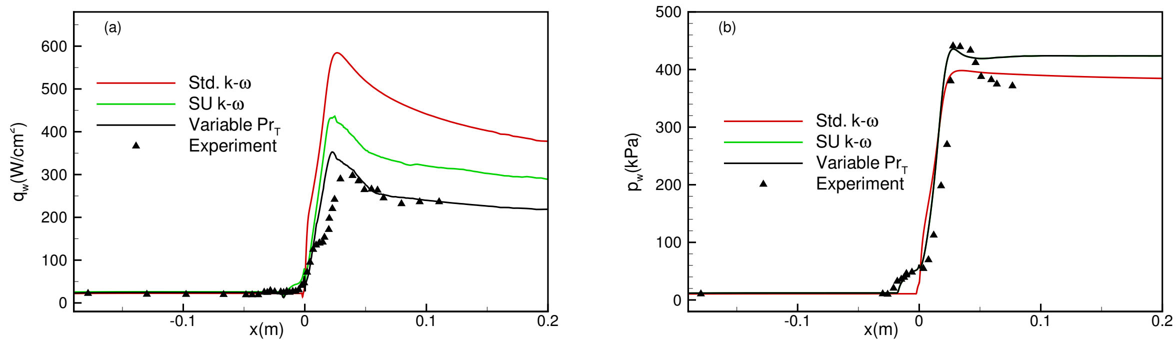

Figure 3. Comparison of (a) Wall heat flux and (b) Surface pressure for $\theta = 33^o$ and $M_\infty = 8.1$ using standard k-ω, shock-unsteadiness modified k-ω and variable Pr_T models with the experimental data of Holden.

than experiment. On the other hand, the variable Pr_T model brings down the post-shock heat transfer dramatically and the results are close to the data presented in the experiments.

Experimental data of the Mach 8, 36 degree compression corner case shows clear indication of flow separation and the shock-unsteadiness k-ω model reproduces this effect. In the following, the pressure contours plot is used to explain the shock structures; see Fig. 4. The separation and reattachment points are marked as S and R respectively. Separation shock meets the reattachment shock wave and generates ramp-induced shock wave in the inviscid flow outside the boundary-layer. This shock-shock interaction is not as prominently predicted by standard k-ω model. At the shock-shock interaction, an expansion wave and high entropy shear-layer are emanated. The expansion waves interact with the compressed boundary-layer on the ramp surface and decrease the surface pressure around $x = 0.035$m which is highlighted in Fig. 5(b).

The surface heat flux is directly influenced by the variation of Pr_T in the reattachment region and in the recovering boundary layer. The prediction of peak heat flux value improves significantly at the reattachment region. The variable Pr_T model also able to match the post-shock heat flux data in the recovery boundary-layer. By comparison, the standard k-ω model with constant turbulent Prandtl number predicts too high a jump in heat flux at the reattachment point, and it overpredicts the data further downstream.

The pressure prediction shows fair comparison with the measurements. The wall pressure computed using the SU k-ω model exhibits a distinct jump due to flow separation, but the separation point is little downstream compared to experiment. The standard k-ω model, on the other hand, predicts a small region pressure plateau and have a small signature of a separation bubble. Once again, the variable Pr_T modification does not have any effect on surface pressure.

The shock pattern computed in the Mach 11 SBLI case is very similar to that of Mach 8, 36 degree

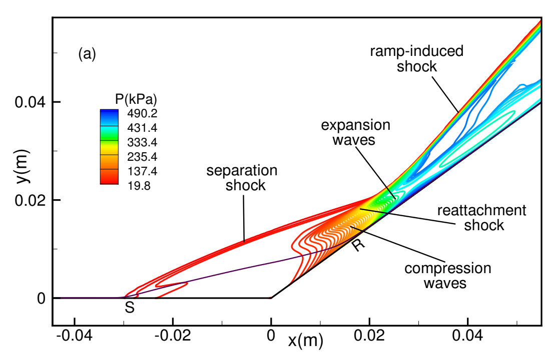

Figure 4. Distribution of computed pressure field for $\theta = 36^o$ and $M_\infty = 8.2$.

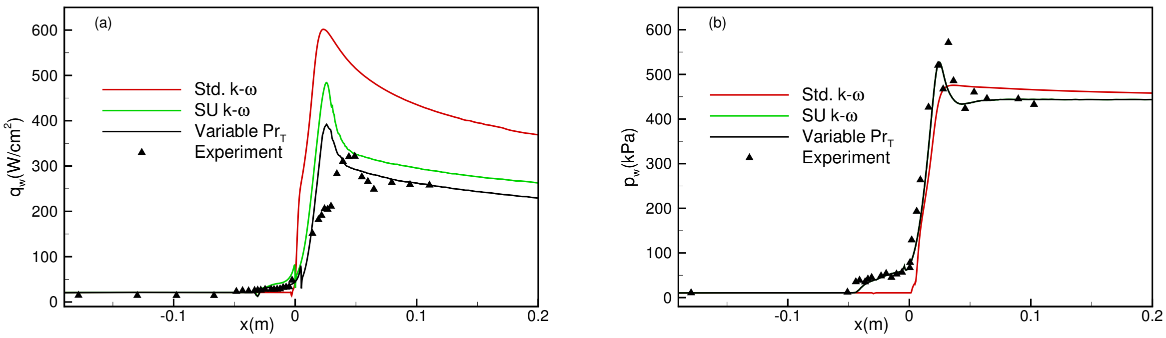

Figure 5. Comparison of (a) Wall heat flux and (b) Surface pressure for $\theta = 36^o$ and $M_\infty = 8.2$ using standard k-ω, shock-unsteadiness modified k-ω and variable Pr_T models with the experimental data of Holden.

case presented before. The separation and ramp induced shocks are identified in the figure 6, along with the limiting stream line showing the extent of the separation bubble. A stronger interaction in this case results in large re-circulation region, with about 120mm between the separation and reattachment points. The density contours plot using SU k-ω model mimic the flow topology of experimental schlieren image very well. Experimental data of wall pressure shows a distinct rise at separation point followed by a pressure plateau in the separation bubble. The simulation results obtained using the shock-unsteadiness k-ω model mimic this trend to some extent. The surface pressure past the reattachment point is also predicted well by the model. We note that the surface pressure is plotted on semi-logarithmic scale so as to enhance the separation point pressure rise at about$x$=-0.8m. By comparison, the standard k-ω model gives a separation bubble much smaller than the experiments, and a steeper pressure rise on reattachment. Here, the interaction of separation shock with the reattachment shock results in a type VI shock-shock interaction; see Fig. 6. A local peak in surface pressure is observed around x=0.05m followed by a sharp decrease due to expansion fan generated at the triple point. This coincides with the regions of peak surface heat flux, and is of direct interest to the present study.

The reattachment shock wave is oriented parallel to the wall in the peak heat transfer region (around $x = 0.05$m). The shock-normal direction is thus oriented towards the wall, such that the turbulent energy transfer in this direction has a direct influence on the surface measurement. Note that the shock-normal component of the heat flux vector is found to be dominant in canonical shock-turbulence interaction, and the variable Prandtl number model is based on the same. It is therefore expected to capture the dominant heat transfer mechanism in the interaction region.

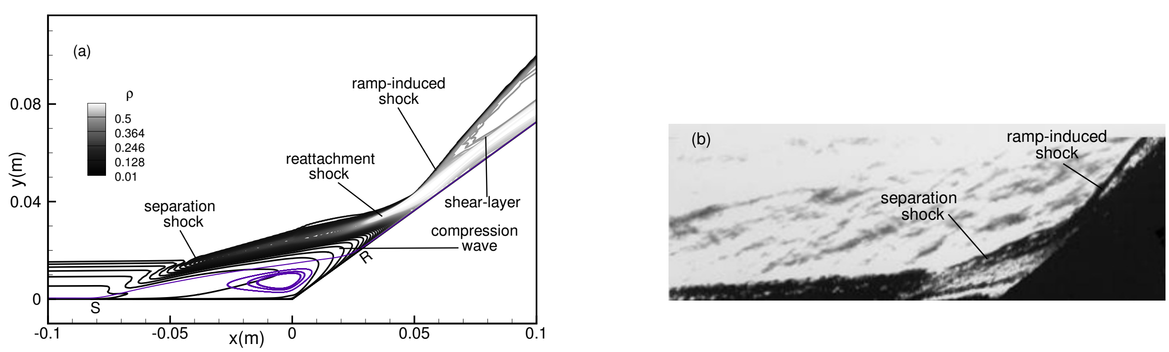

Figure 6. Comparison of (a) computed density contours using SU k-ω model and (b) experimental schlieren image[23] for $\theta = 36^o$ and $M_\infty = 11.3$.

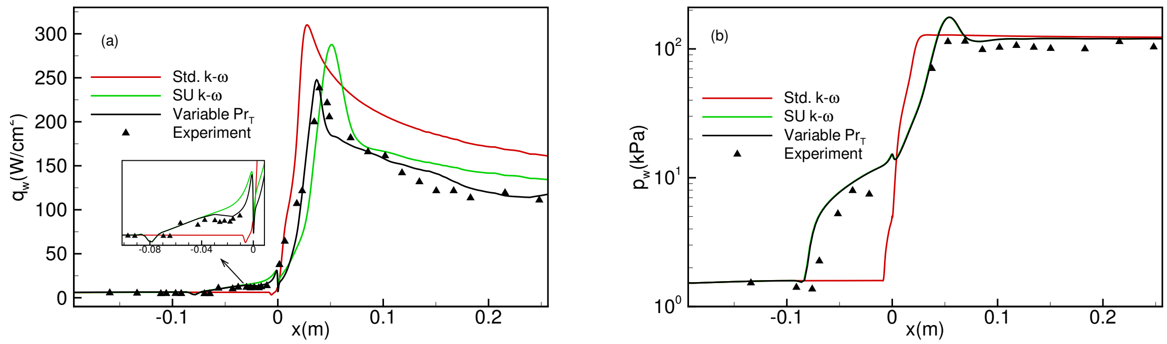

Figure 7. Comparison of (a) Wall heat flux and (b) Surface pressure for $\theta = 36^o$ and $M_\infty = 11.3$ using standard k-ω, shock-unsteadiness modified k-ω and variable Pr_T models with the experimental data of Holden.

The wall heat transfer rate computed in the SBLI region shows the effect of lower turbulent Prandtl number in Fig. 7. Reducing the Pr_T value results in a higher turbulent conductivity $k = \mu_T C_p/Pr_T$. An elevated turbulent conductivity leads to a higher diffusion of heat away from the wall, leading to a lower heat transfer rate on the wall. The predictions are comparable to the experimental measurements in the reattachment region and in the recovering boundary layer. Reducing the eddy viscosity by the shock-unsteadiness correction also gives a similar effect of reduced surface heat flux. By comparison, the standard k-ω model with constant Pr_T overpredicts the peak heat flux by about 30%, and the trends are qualitatively different from that observed in the experiments. The variation of the turbulent Prandtl number based on the shock physics is thus found to significantly improve the heat flux predictions, without any effect on the surface pressure.

B. Oblique shock impinging on a flat plate

The oblique shock impingement case is selected as a second geometry for the validation purpose. Geometric details and the test conditions are presented in section II. The simulation methodology is similar to that presented by Roy, Pathak and Sinha[11] and is not repeated here. The mean dilatation, normalized by incoming boundary layer thikness δ_0=0.014m and freestream velocity, is used to identify shock structure using the SU k-ω model. The incident, induced, separation and reattachment shocks are identified in Fig. 8, along with the limiting stream line showing the extent of the separation bubble. A large negetive value of dilatation represents the highly compressed area by the shock waves. A strong interaction in this case results in a large re-circulation region, with about 0.04m between the separation and reattachment points.

Experimental data of wall pressure shows a distinct rise at the separation point, followed by a pressure plateau in the separation bubble. The simulation results obtained using the shock-unsteadiness k-ω model mimic this trend; see Fig. 9(b). The surface pressure past the reattachment point is also predicted well

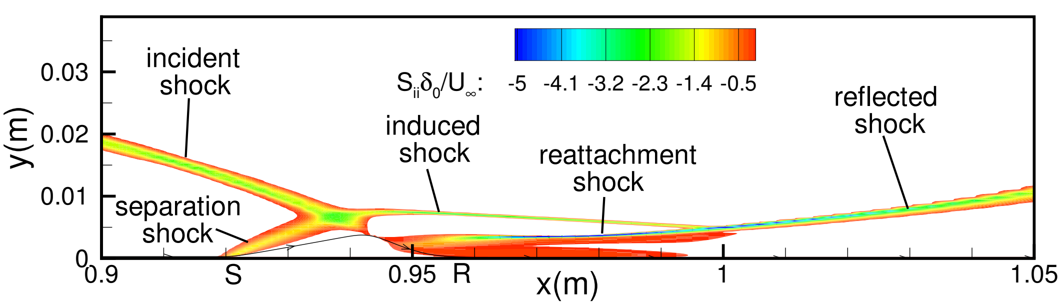

Figure 8. Distribution of normalized mean dilatation using SU k-ω model for $\beta = 20^o$ and $M_\infty = 11.4$.

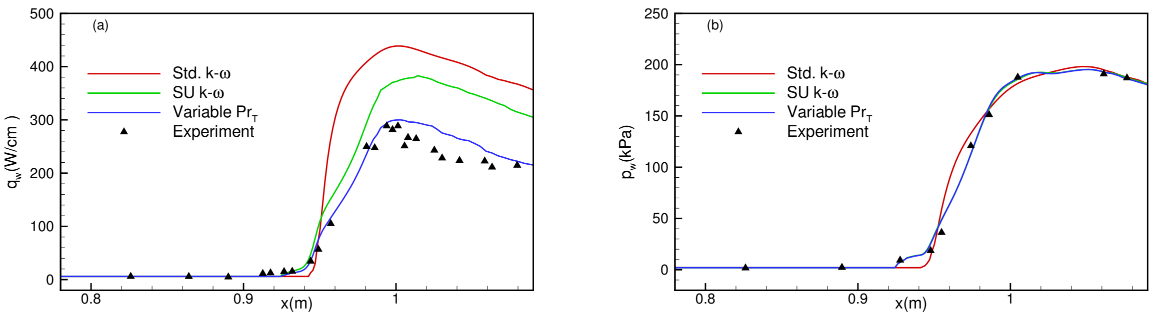

Figure 9. Comparison of (a) Wall heat flux and (b) Surface pressure for $\beta = 20^o$ and $M_\infty = 11.4$ using standard k-ω, shock-unsteadiness modified k-ω and variable Pr_T models with the experimental data of Holden.

by the model. By comparison, the standard k-ω model gives a separation bubble much smaller than the experiments, and a steeper pressure rise on reattachment. Overall, the variable Pr_T model predictions show an excellent comparison with the experimental heat flux measurements in the reattachment region and in the recovering boundary layer. Reducing the eddy viscosity by the shock-unsteadiness correction also gives a reduction in the surface heat flux. By comparison, the standard k-ω model with constant Pr_T overpredicts the peak heat flux by about 50%, and the trends are qualitatively different from that observed in the experiments.

C. Cone-flare

The cone-flare geometry and the boundary-conditions used in the simulations are very similar to those presented by Pasha and Sinha.[15] The present configuration of consits of a 7 degree half-cone and 40 degree flare with respect to the axis. A small symmetry plane is added infront of the cone tip to avoid a stagnation point. Four test cases with progressively increasing Mach numbers are presented here.

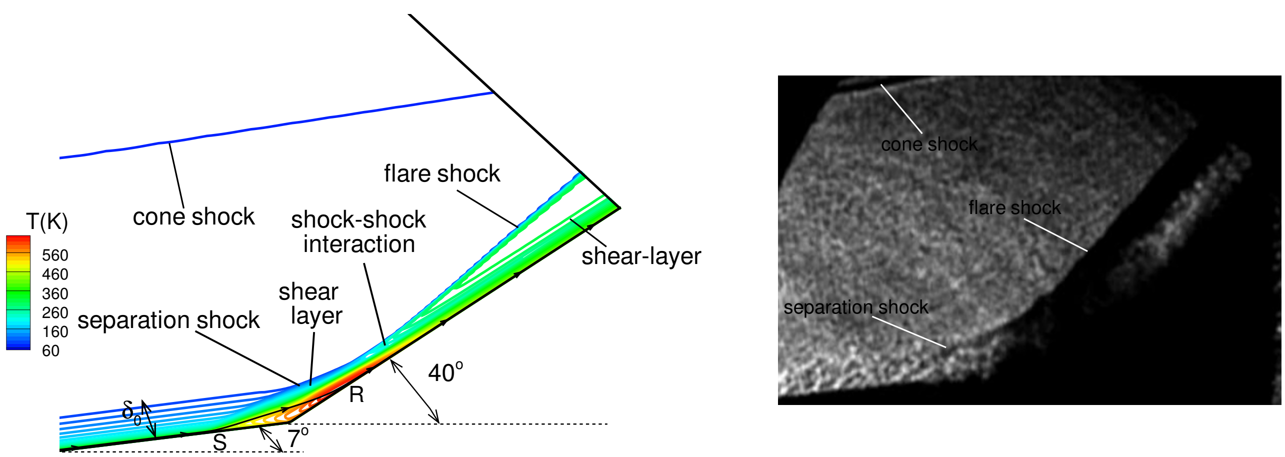

Figure 10. Comparison of computed temperature contours, using (a) SU k-ω model, and (b) experimental schlieren image[23] for $M_\infty = 7$ case.

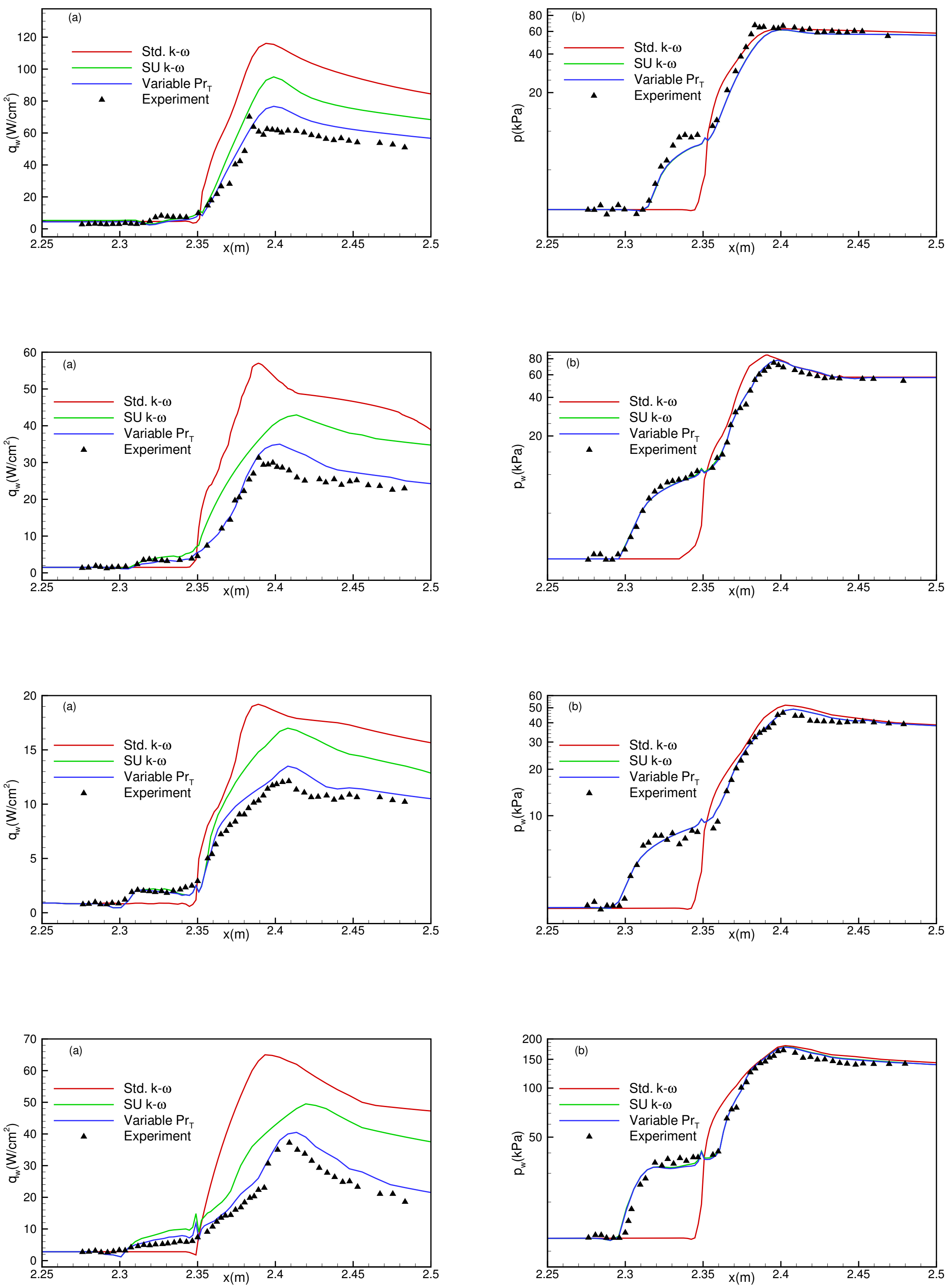

Figure 11. Comparison of (a) Wall heat flux and (b) Surface pressure for $M_\infty = 8, 7, 6, 5$ respectively, using standard k-ω, shock-unsteadiness modified k-ω and variable Pr_T models with the experimental data of Holden.[24]

The flow topology for Mach 8 case is similar to that presented in Ref.,[15] where an intersection of the separation shock with the reattachment shock results in a type VI shock-shock interaction. Expansion waves and high entropy shear-layer are emanated at the shock-shock interaction point; see Ref.[15] for further details. The computed temperature contours for Mach 7 case, using SU k-ω model is compared with the experimental schlieren image in Fig. 10. The shock-shock interaction does not appear to be as clear in experimental schlieren image. A thick boundary layer is formed ahead of the separation shock. The boundary-layer undergoes a compression across the separation shock and bifurcates into two parts. A part of it forms the separated region and part of it flows above separation bubble and further gets compressed across reattachment shock. The shock structure for other two cases are very similar to those described above and are not presented here.

The variationof surface properties are shown in Figs. 11 for all the four test cases.The standard k-ω model predicts a delayed initial pressure rise as compared to the experiment and predicts a smaller separation bubble which is distance between the separation point S and reattachment point R. The SU k-ω model on the other hand mimics the experimental measurements closely for ll the test cases. The pressure plateau between the separation and reattachment points is predicted almost accurately, however, it gives a smaller pressure rise at the reattachment location for the stronger Mach 8 interaction case. The wall pressure drops slighly across the expansion waves after the reattachment region; see Fig. 4 and matches with experiment far downstream.

The wall heat transfer rate computed in the interaction region shows the effect of lower turbulent Prandtl number clearly. The predictions are comparable to the experimental measurements in the reattachment region and in the recovering boundary layer. The heat flux trend inside the separated region is matching the experimental data for higher Mach numbers (Mach 8 and 7), however, there is a dip in the heat flux value for lower Mach numbers just ahead of the reattachment point. Reducing the eddy viscosity by the shock-unsteadiness correction also gives a similar effect of reduced surface heat flux. By comparison, the standard k-ω model with constant Pr_T overpredicts the peak heat flux by about 50 % and the trends are qualitatively different from that observed in the experiments. The variation of the turbulent Prandtl number based on the shock physics is thus found to significantly improve the heat flux predictions, without any effect on the surface pressure.

VI. conclusion

In this paper, we use physical insights from canonical shock-turbulence interaction to extend variable turbulent Prandtl number model of Roy, Pathak and Sinha[11] for hypersonic flows by considering the upstream total temperature fluctuations. The new extension is based on shock-turbulence interaction physics and turbulent boundary layer data sets; both direct numerical simulation and experiment. The effect of upstream total temperature fluctuations on wall heat flux is found to be significant in hypersonic flows compared to supersonic regime.

The new variable Pr_T model is applied, in conjunction with the shock-unsteadiness k-ω turbulence model, to three different geometries at very high-speed. The results are compared with the experimental measurements. It is found that the shock-unsteadiness modification can accurately capture the complex shock topology and the strength of the different shock waves in the flow-field. The low values of the turbulent Prandtl number at the shock waves result in a significant reduction in the surface heat flux prediction. The experimental data is reproduced well, both in terms of the peak heat transfer rate at flow reattachment, as well as the streamwise variation of the surface heat flux in the recovering boundary layer. The computed surface pressure also matches the experimental data better than the standard k-ω model. Thus, the current model gives significant improvement for a wide range of Mach numbers.

Appendix A. Formulation of $\mathbf{A}_{uT}$

The level of temperature and velocity fluctuations in a boundary-layer is not readily available in RANS simulations. To find a relation of A_{uT} with the mean flow variables, we follow the work of Huang, Coleman and Bradshaw.[39] The two length scale of velocity and temperature field in a boundary-layer is defined from the mixing length assumption

$$l_u = \frac{u'}{\partial \overline{u}/\partial y} \tag{A-1}$$

$$l_T = \frac{T'}{\partial\overline{T}/\partial y}. \tag{A-2}$$

This can be combined to give

$$u'\frac{\partial\overline{T}}{\partial y} = cT'\frac{\partial\overline{u}}{\partial y} \tag{A-3}$$

where c is the scaling factor between the two length scale in boundary-layers. Multiplying the above equation by $\rho v'$ and taking a time average at both sides yields

$$\overline{\rho}\overline{u'v'}\frac{\partial\overline{T}}{\partial y} = c\overline{\rho}\overline{v'T'}\frac{\partial\overline{u}}{\partial y}. \tag{A-4}$$

Hence c can be viewed as the ratio of

$$c = \frac{\overline{u'v'}\dfrac{\partial\overline{T}}{\partial y}}{\overline{v'T'}\dfrac{\partial\overline{u}}{\partial y}} = Pr_T \tag{A-5}$$

Thus the velocity and temperature fluctuations expressed as, based on Eqs. (A-1) and (A-2)

$$\frac{T'}{u'} = \frac{1}{Pr_T}\frac{\partial\overline{T}}{\partial\overline{u}} \tag{A-6}$$

Multiplying the denominator and numerator of the above equation by T' and taking the time average gives

$$\frac{\overline{T'^2}}{\overline{u'T'}} = \frac{1}{Pr_T}\frac{\partial\overline{T}}{\partial\overline{u}} \tag{A-7}$$

The temperature gradient with respect to the mean velocity can be found from the definition of total temperature for a mean flow by assuming $\overline{u} >> \overline{v}$ in boundary-layer

$$\overline{T_t} = \overline{T} + \frac{1}{2c_p}\overline{u}^2 \tag{A-8}$$

$$\text{or,}\ \frac{\partial\overline{T}}{\partial\overline{u}} = \frac{\overline{u}}{c_p}\left(\frac{\partial\overline{T_t}}{\partial\overline{T}} - 1\right)^{-1}. \tag{A-9}$$

The above relation simplifies the Eq. A-7 as

$$\frac{\overline{T'^2}}{\overline{u'T'}} = \frac{1}{Pr_T}\frac{\overline{u}}{c_p}\left(\frac{\partial\overline{T_t}}{\partial\overline{T}} - 1\right)^{-1} \tag{A-10}$$

which gives an expression for the function A_{uT}:

$$A_{uT} = -(\gamma-1)M^2\frac{R_{uT}}{Pr_T}\left(\frac{\partial\overline{T_t}}{\partial\overline{T}} - 1\right)^{-1} \tag{A-11}$$

References

[1] Gaitonde, D.V., "Progress in shock wave/boundary layer interactions." *Progress in Aerospace Sciences*, Vol. 72, Jan. 2015, pp. 80-99.

[2] Brown, J.L., "Hypersonic shock wave impingement on turbulent boundary layers: computational analysis and uncertainty," *Journal of Spacecraft and Rockets*, Vol 50, No. 1, 2013, pp. 96-123.

[3] Roy, C.J., and Blottner, F.G., "Review and assessment of turbulence models for hypersonic flows," *Progress in Aerospace Sciences*, Vol. 42, No. 7, 2006, pp. 469-530.

[4]Morkovin, M.V., "Effects of compressibility on turbulent flows," *Mecanique de la Turbulence*,edited by A. Favre, Gordon and Breach, New York, 1964, pp. 367-380.

[5]Wilcox, D.C., Turbulence modeling for CFD. Vol. 2. La Canada, CA: DCW industries, 1998.

[6]Xiao, X., Edwards J.R., Hassan A. H., and Gaffney R.L., "Role of turbulent Prandtl numbers on heat flux at hypersonic Mach numbers," *AIAA Journal*, Vol. 45, No. 4, 2007, pp. 806-813.

[7]Ott, J.D., Donald C.K., and Dash, S.M., "Evaluation of Turbulence Modeling Extensions for the Analysis of Hypersonic Shock Wave Boundary Layer Interactions," *51st AIAA Aerospace Sciences Meeting Including the New Horizons Forum and Aerospace Exposition*, AIAA Paper 2013-0983, Jan. 2013.

[8]Kays, W.M., "Turbulent Prandtl number - where are we?," *Journal of Heat Transfer*, Vol. 116, No. 2, 1994, pp. 284-295.

[9]Quadros, R., Sinha K. and Larsson J., "Turbulent energy flux generated by shock/homogeneous-turbulence interaction," *Journal of Fluid Mechanics*, Vol. 796, June 2016, pp. 113157.

[10]Quadros, R., Sinha K., and Larsson J., "Kovasznay Mode Decomposition of Velocity-Temperature Correlation in Canonical Shock-Turbulence Interaction," *Flow, Turbulence and Combustion*, Vol. 97, No. 3, 2016, pp. 787810.

[11]Roy, S., Pathak, U. and Sinha, K., "Variable Turbulent Prandtl Number Model for Shock/Boundary-Layer Interaction," *AIAA Journal*, Vol. 56, No.1, 2018, pp. 1-14.

[12]Sinha, K., Mahesh K., and Candler, G.V., "Modeling shock unsteadiness in shock/turbulence interaction," *Physics of Fluids*, Vol.15, No. 8, 2003, pp. 2290-2297.

[13]Sinha, K., Mahesh K., and Candler, G.V., "Modeling the effect of shock unsteadiness in shock/turbulent boundary-layer interactions," *AIAA Journal*, Vol. 43, No. 3, 2005, pp. 586-594.

[14]Pasha, A.A., and Sinha K. "Shock-unsteadiness model applied to oblique shock wave/turbulent boundary-layer interaction," *International Journal of Computational Fluid Dynamics*, Vol. 22, No. 8, 2008, pp. 569-582.

[15]Pasha, A.A., and Sinha, K., "Simulation of hypersonic shock/turbulent boundary-layer interactions using shock-unsteadiness model," *Journal of Propulsion and Power*, Vol. 28, No. 1, 2012, pp. 46-60.

[16]Zhang, Z., Gao, Z., Jiang, C., and Lee, C.H., "A RANS model correction on unphysical over-prediction of turbulent quantities across shock wave," *International Journal of Heat and Mass Transfer*, Vol. 106, 2017, pp. 1107-1119.

[17]Emami, B., Bussmann, M., and Tran, H., "Application of realizability and shock unsteadiness to k-ϵ simulations of under-expanded axisymmetric supersonic free jets," *Journal of Fluids Engineering*, Vol. 132, No. 4, 2010, pp. 04-11.

[18]Sinha, K., and Balasridhar, S. J., "Conservative Formulation of the k-ϵ Turbulence Model for Shock-Turbulence Interaction," *AIAA Journal*, Vol. 51, No. 8, 2013, pp. 1872-1882.

[19]Raje, P., and Sinha, K., "A physically consistent and numerically robust k-ϵ model for computing turbulent flows with shock waves," *Computers & Fluids*, Vol. 136, 2016, pp. 35-47. doi: 10.1016/j.compfluid.2016.05.026

[20]Schulein, E., "Skin friction and heat flux measurements in shock/boundary layer interaction flows," *AIAA Journal*, Vol. 44, No. 8, 2006, pp. 1732-1742. doi: 10.2514/1.15110

[21]Leschziner, M. A., Batten, P., and Loyau, H., "Modelling shock-affected near-wall flows with anisotropy-resolving turbulence closures," *International Journal of Heat and Fluid Flow*, Vol. 21, No. 3, 2000, pp. 239-251.

[22]Duan, L., Beekman, I., and Martin, M.P., "Direct numerical simulation of hypersonic turbulent boundary layers with varying free stream Mach number," *AIAA Paper* No. 353, 2010.

[23]Holden, M.S., Wadhams, T., MacLean, M., and Mundy, E., "Experimental studies of shock wave/turbulent boundary layer interaction in high Reynolds number supersonic and hypersonic flows to evaluate the performance of CFD codes," 40th *Fluid Dynamics Conference and Exhibit*, Chicago, Illinois 28 June - 01 July 2010.

[24]Holden, M. S., Wadhams, T., MacLean, M., and Dufrene, A., Measurements in Regions of Shock Wave/Turbulent Boundary Layer Interaction from Mach 4 to 10 for Open and Blind Code Evaluation/Validation," 21st AIAA *Computational Fluid Dynamics Conference*,San Diego, California 24-27 June 2013.

[25]Marvin, J. G., Brown, J. L., and Gnoffo, P. A., "Experimental database with baseline CFD solutions: 2-D and axisymmetric hypersonic shock-wave/turbulent-boundary-layer interactions," NASA Ames Research Center, NASA TM-2013-216604, Moffett Field, CA, 2013.

[26]Forsythe, J., Hoffmann, K., and Damevin, H.M., "An assessment of several turbulence models for supersonic compression ramp flow," 29th AIAA, *Fluid Dynamics Conference*, Albuquerque, New Mexico 15-18 June 1998.

[27]Coakley, T., and Huang, P., "Turbulence modeling for high speed flows," *30th Aerospace Sciences Meeting and Exhibit*, Reno, Nevada 6-9 January 1992.

[28]MacCormack, R.W., and Candler, G.V., "The solution of the Navier-Stokes equations using Gauss-Seidel line relaxation," *Computers & fluids*, Vol. 17, No. 1, 1989, pp. 135-150.

[29]Sinha, K., and Candler, G.V., "Convergence improvement of two-equation turbulence model calculations," *29th AIAA Fluid Dynamics Conference*, AIAA Paper 1998-2649, June 1998.

[30]Wright, M.J., Candler, G.V, and Bose, D., "Data-parallel line relaxation method for the Navier-Stokes equations," *AIAA Journal*, Vol. 36, No. 9, 1998, pp. 1603-1609.

[31]Menter, F.R., "Two-equation eddy-viscosity turbulence models for engineering applications," *AIAA Journal*, Vol. 32, No. 8, 1994, pp. 1598-1605.

[32]Sinha, K., "Evolution of enstrophy in shock/homogeneous turbulence interaction," *Journal of Fluid Mechanics*, Vol. 707, 2012, pp. 74-110.

[33]Larsson, J., Bermejo-Moreno, I., and Lele, S. K., "Reynolds-and Mach-number effects in canonical shock-turbulence interaction," *Journal of Fluid Mechanics*, Vol. 717, 2013, pp. 293-321.

[34]Guarini, S.E., Moser, R.D., Shariff, K., and Wray, A., "Direct numerical simulation of a supersonic turbulent boundary layer at Mach 2.5," *Journal of Fluid Mechanics*, Vol. 414, 2000, pp. 1-33.

[35]Pirozzoli, S., Grasso, F., and Gatski, T.B ,"Direct numerical simulation and analysis of a spatially evolving supersonic turbulent boundary layer at M= 2.25," *Physics of fluids*, Vol. 16, No. 3, 2004, pp. 530-545.

[36]Gaviglio, J., “Reynolds analogies and experimental study of heat transfer in the supersonic boundary layer,” *International journal of heat and mass transfer*, Vol. 30, No. 5, 1987, pp. 911-926.

[37]Pathak, U., Roy, S., and Sinha, K., “A phenomenological model for turbulent heat flux in high-speed flows with shock-induced flow separation,” *Journal of Fluids Engineering*, Vol. 140, No. 5, 2018, pp. 1-9.

[38]Veera, V.K., and Sinha, K., “Modeling the effect of upstream temperature fluctuations on shock/homogeneous turbulence interaction,” *Physics of fluids*, Vol. 21, No. 2,2009.

[39]Huang, P.G., Coleman, G.N., and Bradshaw, P., “Compressible turbulent channel flows: DNS results and modelling,” *Journal of Fluid Mechanics*, Vol. 305, 1995, pp. 185-218.